Metallic Reflection Spectra of K_3C_{60}

Y. Iwasa, K. Tanaka, T. Yasuda, and T. Koda
Department of Applied Physics, The University of Tokyo, Tokyo 113, Japan

S. Koda
Department of Chemical Engineering, The University of Tokyo, Tokyo 113, Japan

(Received 13 April 1992)

Optical reflectivity spectra were measured for the superconducting fulleride K_3C_{60} and for pristine C_{60} single crystals in the wavelength region from infrared to ultraviolet. High-quality samples of K_3C_{60} with flat surfaces were grown for this purpose by cosublimation of both C_{60} and potassium metal. A sharp plasma edge was found at 0.73 eV in the reflection spectra of K_3C_{60}. A quantitative discussion is given on the conduction band structures based on the band parameters derived from a spectral shape analysis in terms of the Drude-Lorentz model.

PACS numbers: 74.70.Ya, 78.20.Ci

Metallization in alkali-metal-doped C_{60} has attracted great interest [1], leading to the discovery of superconductivity in stoichiometric compounds A_3C_{60} (A = K,Rb,Cs and their mixtures) [2-4] and Ca_5C_{60} [5]. In order to elucidate the normal-state properties of A_3C_{60}, a variety of experimental works have been done on photoemission [6-8], NMR [9], far-infrared spectra [10], and electronic transport [11]. However, optical spectra that are crucial for the study of electronic structures have not been well explored except for high energies [12,13]. In this Letter we present optical reflection spectra of C_{60} single crystals and K_3C_{60} polycrystalline films, which have been prepared by a so-called "cosublimation" method. In K_3C_{60}, a metallic reflection band was found to show the plasma edge at 0.73 eV. This spectrum is interpreted well by the Drude-Lorentz model. The derived band parameters indicate that, though the bandwidth of K_3C_{60} is as narrow as 0.3 eV, the observed features of the spectrum are reasonably accounted for within the framework of a band picture.

Pristine C_{60} powders were synthesized by the Kratchmer-Huffman method [14]. The purity of C_{60} was confirmed to be more than 99% by infrared spectroscopy. C_{60} single crystals were grown from slow evaporation of C_{60} powder in a sealed quartz tube, following the procedure described in the literature [15]. The obtained crystals have typical dimensions of $1\times1\times0.5$–$2\times3\times1$ mm^3. The crystal structure was confirmed to be fcc by an x-ray analysis.

In order to obtain high-quality K_3C_{60} samples, we employed a cosublimation method, known to be useful in the single-crystal growth of organic charge-transfer compounds [16]. In this method, C_{60} and potassium are simultaneously vaporized and allowed to react in the vapor phase. According to a simple calculation taking account of the ionization and Madelung energies, the K_3C_{60} phase is the most stable form among various K_xC_{60} compounds (x = 0,3,4,6) [17]. It is expected therefore that high-quality K_3C_{60} is obtained by maintaining the pressure of potassium at a proper level.

The problem is how to reduce the vapor pressure of potassium, which is much higher than the pressure of C_{60} at the same temperature. To resolve this problem, we used a reaction cell which is schematically depicted in the inset of Fig. 1. The C_{60} powder of about 20 mg was loaded at the one end of a 10-mm-diam quartz tube. A piece of potassium metal was placed in a smaller inner tube, in a He glove box. The amount of potassium was about 1.5 times larger than the stoichiometric weight. This cell was sealed after evacuation to 2×10^{-6} torr, and set in a furnace with a temperature gradient, so as to keep the C_{60} part at 600 °C and the other end at about 350 °C. The potassium vapor pressure at the middle part of the cell is determined by the diffusion of the vapor through the cold part of the tube. In this way, the vapor pressures of both C_{60} and potassium metal were suitably maintained in the tube to form cosublimed black powders on the inside wall in the middle part of the tube. (If we did not use the inner tube, the potassium vapor pressure became so high that C_{60} powders at the right end of the tube were doped without being sublimed.) The left side of the tube was colored brown due to the chemical reaction of the exces-

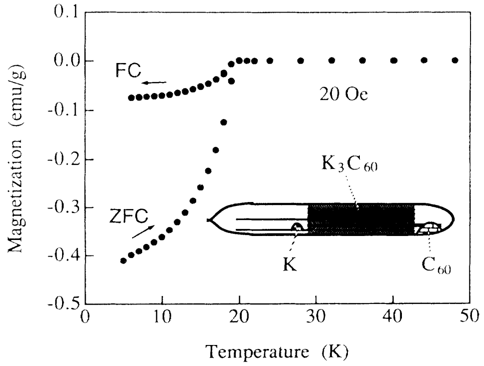

FIG. 1. Temperature dependence of the zero-field-cooled (ZFC) and field-cooled (FC) dc magnetization of K_3C_{60} with an applied magnetic field of 20 Oe. Inset: The reaction cell used.

sive potassium vapor and quartz. After reaction for about 24 h, polycrystalline materials, including powders and several pieces of films or flakes with typical dimensions of $\sim 2\times 2$ mm^2, were obtained in the middle part of the quartz tube. These flakes scraped from the tube had shiny flat surfaces on the side which had attached to the inner wall of the tube.

To characterize the quality of flake samples thus obtained, we show the measured temperature dependence of magnetization at 20 Oe. Superconductivity was confirmed to occur at $T_c \sim 19$ K as shown in Fig. 1. The volume fraction of superconductivity was estimated to be about 50% from the shielding effect. The bulk superconductivity indicates that cosublimed samples are mainly composed of K_3C_{60}. We also measured the Raman spectra of the flakes. A strong Raman peak of the A_g mode was observed at 1445 cm^{-1} which is known to be characteristic of K_3C_{60} [1,18]. A weak shoulder structure of the pristine C_{60} was also found at 1468 cm^{-1}. Other peaks were observed in this region, excluding the existence of overdoped components. The Raman data clearly show that our sample is predominantly composed of K_3C_{60}, containing a slight amount of C_{60} as an impurity. From the relative Raman intensity of K_3C_{60} and C_{60}, the concentration of C_{60} is estimated to be on the order of several percent.

Although the films have a polycrystalline structure, they have a sufficiently flat surface to make reliable optical reflection measurements. Since K_3C_{60} has an isotropic crystal structure, the polycrystallinity does not seriously affect the quality of the reflection spectra. A more careful adjustment of growth conditions may lead to the growth of single crystals of K_3C_{60} and other fullerides by this cosublimation method.

Reflection spectra were measured at room temperature. For C_{60} single crystals, the measurement was done in air. For K_3C_{60}, which is unstable in air, film samples were loaded in a glove box into a vacuum cell with an optical window, and then the cell was evacuated down to 3×10^{-6} torr. The reflection measurements were made in the wavelength region from 16 to 0.19 μm. Absolute reflectivities were determined with an accuracy of 15% error by microscopic spectroscopy.

Figure 2 shows reflection spectra of K_3C_{60} and C_{60}. Reproducible reflectivity spectra were obtained for K_3C_{60} samples obtained from different batches, ensuring a good sample quality. For C_{60} single crystals, the spectrum was taken on the as-grown (111) surface. Several important features should be noticed in the spectra. Four strong peaks observed above 2 eV are in agreement with features reported in the absorption spectra for evaporated C_{60} thin films [14]. These characteristic features remain essentially unchanged in K_3C_{60}. In the lower energy region, however, a drastic change of the spectrum takes place by doping: For pristine C_{60} crystal the spectrum is flat except for the sharp peaks at 0.1465 eV (1182 cm^{-1}) and 0.1770 eV (1428 cm^{-1}) due to the well-known vibration modes [12]. In contrast, a metallic reflection with a sharp plasma edge at 0.73 eV was found for K_3C_{60}. Discussions on this structure will be given later. Second, a new peak was found to appear at 0.91 eV in K_3C_{60}, which was absent in the pristine C_{60}. Another interesting feature is the change in the vibration modes by doping. In K_3C_{60}, only one peak is observed at 0.1691 eV (1364 cm^{-1}). This peak corresponds to an intramolecular vibration mode at 1428 cm^{-1} in C_{60}. The width of this peak in K_3C_{60} is 17 cm^{-1} which is considerably larger than the width (7 cm^{-1}) of the corresponding structure in C_{60}. This large shift and broadening are attributable to the interaction between the intramolecular vibration and the conduction electrons.

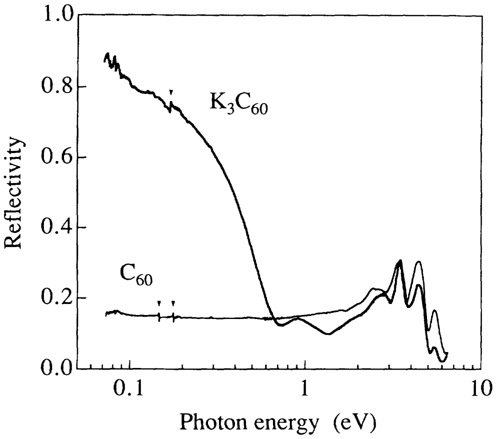

FIG. 2. Reflectivity spectra of K_3C_{60} (thick solid line) and C_{60} (thin solid line). Vibration modes are marked by arrows.

The main feature of the spectrum in K_3C_{60} is obviously the metallic reflection appearing in the infrared region. To get quantitative information on the conduction band of K_3C_{60}, we made a spectral shape analysis in terms of the Drude-Lorentz model. In this model, the dielectric constant $\varepsilon(\omega)$ is written as follows:

$$\varepsilon(\omega)=\varepsilon_\infty-\frac{\omega_p^2}{\omega(\omega+i\gamma_p)}+\frac{f_L\omega_L^2}{\omega_L^2-\omega^2-i\gamma_L\omega},$$

where ε_∞ is the dielectric constant at high energy, ω_p the plasma energy, γ_p the damping constant, and f_L, ω_L, and γ_L the oscillator strength, energy, and damping factor of the Lorentz oscillator, respectively. The best-fit curve is plotted in Fig. 3(a) by a thin solid line. The fitting parameters are listed in the inset. The overall agreement is fairly good, and the following picture of the conduction band can be drawn from these parameters.

Assuming a triply degenerate parabolic conduction band, the electron effective mass m^* is calculated to be $2.4m_0$ from the relation $\omega_p^2=ne^2/\varepsilon_0 m^*$. Here, the carrier concentration n was assumed to be 4.1×10^{21} cm^{-3}, i.e., three carriers per C_{60} molecule. The m^* value leads to a bandwidth of 0.3 eV and Fermi energy of 0.2 eV, and the

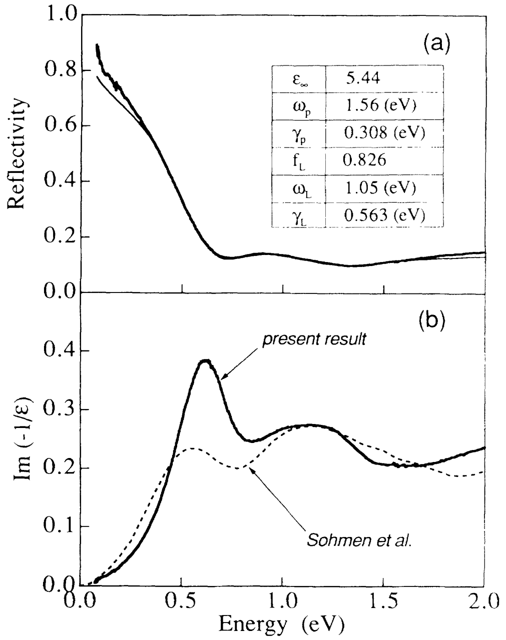

FIG. 3. (a) Experimental and calculated reflectivity spectra of K_3C_{60}, shown by a thick solid line and thin solid line, respectively. The fitting parameters are listed in the inset. (b) Solid line: $\mathrm{Im}(-1/\varepsilon)$ spectrum for K_3C_{60} calculated from the reflectivity spectrum by the Kramers-Kronig transformation. Dashed line: EELS for K_xC_{60} ($x=2.5$) after Sohmen, Fink, and Kratchmer [21], plotted in arbitrary units.

TABLE I. Comparison of the band parameters obtained from several experiments on normal-state properties. χ is the magnetic susceptibility; m^*, conduction-band effective mass; $N(\varepsilon_F)$, density of states per C_{60}; ε_F, Fermi energy in eV.

Expt.	m^*/m_0	$N(\varepsilon_F)$	ε_F	Reference
Optical	2.4	23	0.2	Present
NMR		20		[9]
χ	4.5	22		[19]

density of states at the Fermi energy is estimated to be $N(E_F)=23\ \mathrm{eV}^{-1}$ per C_{60} molecule. The obtained parameters are listed in Table I together with previous results obtained by other groups.

The optically determined parameters compare favorably with values derived before from other low-energy experiments such as NMR [9], electronic transport [11], and magnetic susceptibility [19]. For an example, from NMR data, it has been reported that $N(E_F)\sim 20\ \mathrm{eV}^{-1}$ per C_{60} molecule [9]. The agreement is good, considering the difference of the energy scales in the measurements. The optical parameter is an average over the whole conduction band, while the magnetically determined parameters are determined from the shape of the conduction band just at the Fermi level. These results indicate that metallic properties of K_3C_{60} are consistently explained by a half-filled conduction band model.

From the estimated damping parameter γ_p, the dc conductivity is calculated to be $\sigma\sim 1\times 10^3$ S/cm, which is of the same order as that from the dc resistivity measurements ($\sigma\sim 5\times 10^2$ S/cm) [1,11]. Using the Fermi velocity $v_F\sim 2\times 10^5$ m/s derived from the effective mass, the mean free path was estimated to be $l\sim 3.6$ Å, which is considerably smaller than the lattice constant $a=14.25$ Å of K_3C_{60}. This value is also consistent with the transport data [11], indicating the breakdown of the free-electron picture assumed in the Drude model. Although the band parameters derived from this model still have a semiquantitative meaning, K_3C_{60} is close to the metal-insulator boundary at room temperature. More elaborate experimental and theoretical studies are needed to settle the problems such as a deviation from the Drude picture or the existence of a pseudo gap state [8].

Let us examine the present optical data in comparison with the results from band calculations and previous spectroscopic data. For example, Erwin and Pickett have estimated the plasma energy as $\omega_p=1.2$ eV based on a band calculation [20], which is in reasonable agreement with the present result of $\omega_p=1.56$ eV. According to the band picture, the reflection peak at 0.91 eV in K_3C_{60} is assigned to the interband absorption between the lower two conduction bands, which originate from the t_{1u} and the t_{1g} molecular levels, respectively. The appearance of this transition in K_3C_{60} is attributed to the introduction of electrons to the t_{1u} level upon doping. This band has been also observed by Pichler *et al.* [12] at 1.3 eV in the absorption measurement.

It is also interesting to compare the present optical data with the electron-energy-loss spectra (EELS) for K_xC_{60} ($0<x<6$) by Sohmen, Fink, and Kratchmer [21]. Figure 3(b) shows the $\mathrm{Im}(-1/\varepsilon)$ spectrum for K_3C_{60} which has been calculated from the reflection spectrum by the Kramers-Kronig transformation. Overall features of the $\mathrm{Im}(-1/\varepsilon)$ spectrum are quite similar to those of the EELS for K_xC_{60} ($x=2.5$) [21] shown by the dashed line. Sohmen, Fink, and Kratchmer did not make a clear-cut interpretation on the lower energy peak. However, according to the reflection spectrum in Fig. 3(a) and above-mentioned discussions, the peaks at 0.62 eV are attributable to the excitation of carrier plasmon, and the peak at 1.13 eV to the interband transition, respectively.

In conclusion, we have grown high-quality K_3C_{60} samples by a cosublimation method, which enabled us to measure reliable reflectivity spectra for this compound. Observed features of the spectra can be consistently interpreted in terms of the plasma edge and a doping-induced interband transition. The effective mass of the conduction band was obtained to be $2.4m_0$.

We thank Professor H. Suematsu, Professor M. Gonokami, Dr. Y. Murakami, and Dr. Y. Ishii for their experimental help. We are also grateful to Professor Y. Tokura and T. Arima for valuable discussions.

---

[1] R. C. Haddon *et al.*, Nature (London) **350**, 320 (1991).
[2] A. F. Hebbard *et al.*, Nature (London) **350**, 600 (1991).
[3] M. J. Rosseinsky *et al.*, Phys. Rev. Lett. **66**, 2830 (1991).
[4] R. M. Fleming *et al.*, Nature (London) **352**, 787 (1991).
[5] A. R. Kortan *et al.*, Nature (London) **355**, 529 (1992).
[6] P. J. Benning *et al.*, Science **252**, 1417 (1991).
[7] C. T. Chen *et al.*, Nature (London) **352**, 603 (1991).
[8] T. Takahashi *et al.*, Phys. Rev. Lett. **68**, 1232 (1992).
[9] R. Tycko *et al.*, Science **253**, 884 (1991).
[10] L. D. Rotter *et al.*, Nature (London) **355**, 532 (1992).
[11] T. T. Palstra, R. C. Haddon, A. F. Hebard, and J. Zaanen, Phys. Rev. Lett. **68**, 1054 (1992).
[12] T. Pichler, M. Matus, J. Kurti, and H. Kuzmany, Solid State Commun. **81**, 859 (1992).
[13] V. I. Srdanov *et al.*, Chem. Phys. Lett. **192**, 243 (1992).
[14] W. Kratchmer, L. D. Lamb, K. Fostiropoulos, and D. R. Huffman, Nature (London) **347**, 354 (1991).
[15] R. L. Meng *et al.*, Appl. Phys. Lett. **59**, 3402 (1991).
[16] Y. Iwasa *et al.*, Phys. Rev. B **42**, 2374 (1990).
[17] R. M. Fleming *et al.*, Nature (London) **352**, 701 (1991).
[18] M. G. Mitch, S. J. Chase, and J. S. Lannin, Phys. Rev. Lett. **68**, 883 (1992).
[19] W. H. Wong *et al.*, Europhys. Lett. **18**, 79 (1992).
[20] S. C. Erwin and W. E. Pickett, Science **254**, 842 (1991).
[21] E. Sohmen, J. Fink, and W. Kratchmer, Europhys. Lett. **17**, 51 (1992).

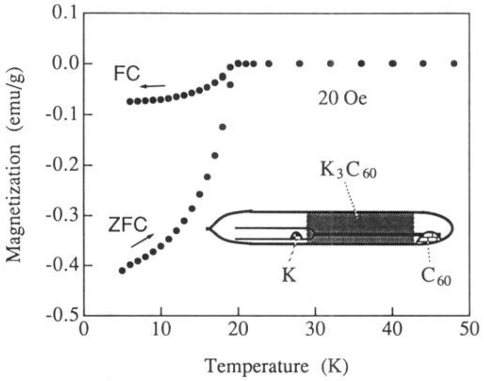

FIG. 1. Temperature dependence of the zero-field-cooled (ZFC) and field-cooled (FC) dc magnetization of K_3C_{60} with an applied magnetic field of 20 Oe. Inset: The reaction cell used.